Solution Structure of Reduced Plastocyanin from the Blue-Green Alga *Anabaena variabilis*[†,‡]

Ulla Badsberg,[§] Anne Marie M. Jørgensen,[§] Henrik Gesmar,[§] Jens J. Led,*[,§] Jan M. Hammerstad,[||] Lise-Lotte Jespersen,[||] and Jens Ulstrup*[,||]

Department of Chemistry, University of Copenhagen, The H. C. Ørsted Institute, Universitetsparken 5, DK-2100 Copenhagen Ø, Denmark, and Chemistry Department A, Building 207, The Technical University of Denmark, DK-2800 Lyngby, Denmark

Received March 13, 1996[⊗]

ABSTRACT: The three-dimensional solution structure of plastocyanin from *Anabaena variabilis* (*A.v.* PCu) has been determined by nuclear magnetic resonance spectroscopy. Sixty structures were calculated by distance geometry from 1141 distance restraints and 46 dihedral angle restraints. The distance geometry structures were optimized by simulated annealing and restrained energy minimization. The average rms deviation from the mean structure for the 20 structures with the lowest total energy is 1.25 Å for the backbone atoms and 1.75 Å for all heavy atoms. Overall, the global tertiary fold of *A. v.* PCu resembles those of other plastocyanins which have been structurally characterized by X-ray diffraction and NMR methods. This holds even though *A.v.* PCu is longer than any other known plastocyanins, contains far less invariant amino acid residues, and has an overall charge that differs considerably from those of other plastocyanins ($+1$ *vs* -9 ± 1 at pH ≥ 7). The most striking feature of the *A.v.* PCu structure is the absence of the β-turn, formed at the remote site by residues (58)−(61) in most higher plant plastocyanins. The displacement caused by the absence of this turn is compensated for by an extension of the small helix [from Ala53(51) to Ser60(58) in *A.v.* PCu] found in other plastocyanins. Moreover, the extra residues of *A.v.* PCu from Pro77 to Asp79 form an appended loop. These two features allow *A.v.* PCu to retain almost the same global fold as observed in other plastocyanins. From a comparison with the structures of other plastocyanins it is concluded that the lack of negatively charged residues at the remote site, rather than the specific structure of *A.v.* PCu, is the main reason for the failure of the remote site of this plastocyanin to function as a significant electron transfer site.

Plastocyanins are small (from 97 to 105 amino acids) copper proteins (Malkin & Malmström, 1970) essential in the electron transfer chain of photosynthetic organisms, where it is a mobile electron carrier from the membrane-bound cytochrome b_6/f complex to the primary donor P700 of photosystem I (Haehnel, 1984; Wolk, 1980). Well-resolved three-dimensional structures of plastocyanins from several plants and algae have been elucidated (Colman et al., 1978; Guss & Freeman, 1983; Guss et al., 1986; Moore et al., 1988a, 1991; Bagby et al., 1990, 1994; Collyer et al., 1990; Redinbo et al., 1993). In addition, binding sites and electron transfer kinetics have been investigated in considerable detail (Bueko-Betts et al., 1985; Jackman et al., 1987a,b; McGinnis et al., 1988; Rush et al., 1988; He et al., 1991; Christensen et al., 1992; Dennison et al., 1993).

Platocyanins are of special interest because they appear to exhibit well-defined binding sites for inorganic redox partners and for other electron transfer proteins, cytochrome *f* and P700 in particular (Boulter et al., 1977; Sykes, 1985, 1991; Gross, 1993). The structure−function relationships of plastocyanins have, therefore, been the subject of intense investigations. Studies of the interaction and electron transfer kinetics of plastocyanins with small inorganic complexes (McGinnis et al., 1986, 1988; Jackman et al., 1987a,b; Pladziewicz & Brenner, 1987; Christensen et al., 1990c) indicate that two electron transfer sites are present. One site (the adjacent site) is hydrophobic and located approximately 6 Å from the copper center near the surface of the molecule, on what has been dubbed the "north side" of the molecule. The other site (the remote site) is about 15 Å from the copper center and located on the "east side" of the molecule. Competitive electron transfer *through* the protein can be ascribed to a subtle combination of electronic and structural properties of PCu.[1] A specific electron tunnel route, Cu−Cys(84)−Tyr(83), thus leads from the Cu atom to the central

[†] This work was supported by the Danish Natural Science Research Council, J. Nos. 9400903, 11-9585, and 11-0393, the Danish Technical Research Council, J. No. 9400446, the Ministry of Industry, J. No. 85886, Julie Damm's Studiefond, and Direktør Ib Henriksens Fond.

[‡] Coordinates of the 20 refined structures and the NMR-derived restraints have been deposited in the Brookhaven Protein Data Bank (PDB ID codes 1NIN and R1NINMR, respectively).

* Authors to whom correspondence should be addressed.

[§] University of Copenhagen.

[||] The Technical University of Denmark.

[⊗] Abstract published in *Advance ACS Abstracts,* May 1, 1996.

[1] Abbreviations: NMR, nuclear magnetic resonance; COSY, two-dimensional correlated spectroscopy; DQF-COSY, double-quantum-filtered COSY; TOCSY, total correlation spectroscopy; DANTE, delays alternating with nutation for tailored excitation; DIPSI, decoupling in the presence of scalar interactions; 2D, two dimensional; FID, free induction decay; GARP, globally optimized alternating-phase rectangular pulses; NOE, nuclear Overhauser enhancement; NOESY, NOE correlated spectroscopy; HMQC, heteronuclear multiple-quantum coherence; TPPI, time-proportional phase increments; ppm, parts per million; $d_{\alpha N}(i,j)$, distance and corresponding NOE connectivity between the αCH proton on residue *i* and the NH proton on residue *j* [$d_{NN}(i,j)$, $d_{\beta N}(i,j)$, $d_{\alpha N} = d_{\alpha N}(i,i+1)$, $d_{NN} = d_{NN}(i,i+1)$, $d_{\beta N} = d_{\beta N}(i,i+1)$, defined accordingly]; $^3J_{H_\alpha H_N}$, three-bond coupling between an α proton and an amide proton; RMD, restrained molecular dynamics; rms, root mean square; rmsd, root mean square deviation; DGSA, distance geometry simulated annealing; *A.v.*, *Anabaena variabilis*; PCu, plastocyanin.

S0006-2960(96)00621-6 CCC: $12.00

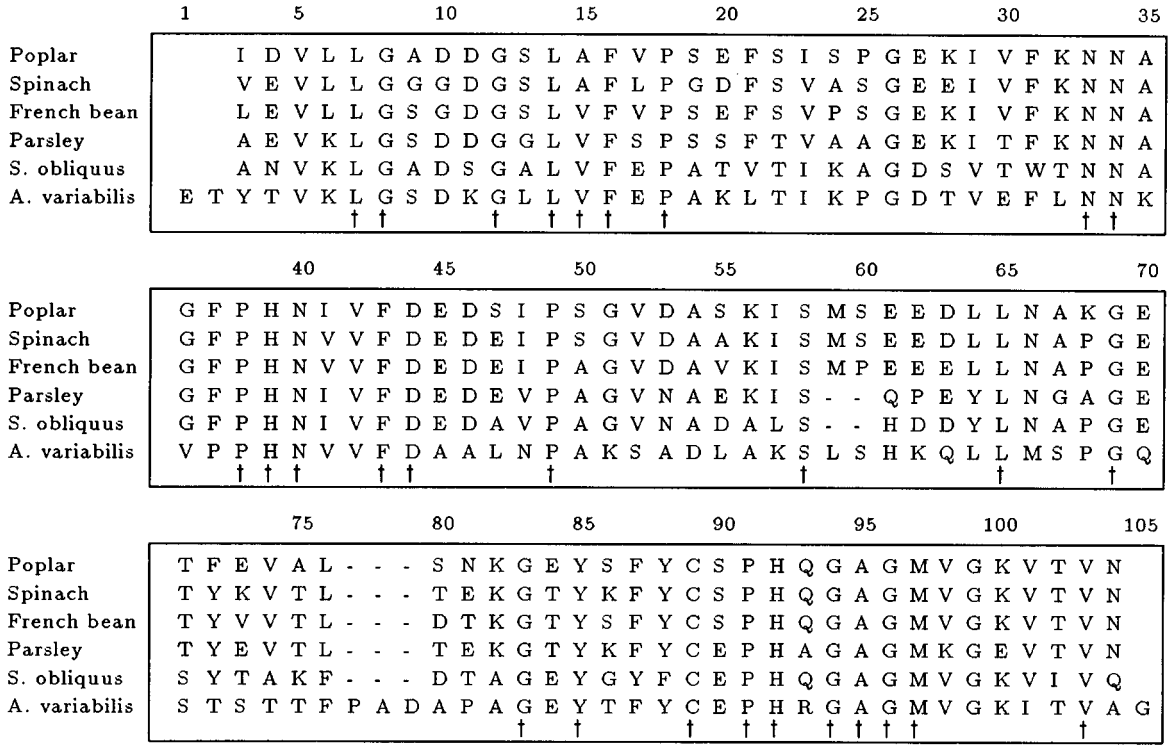

FIGURE 1: Plastocyanin amino acid sequences. A † indicates amino acid residues which are invariant in all plastocyanins.

remote site residue, Tyr(83) (Christensen et al., 1990a). The electron tunnel factor of this route is about 2% of the value for the adjacent site tunnel route, while all other routes are much less facile. In addition, the remote site consists of two patches of acidic residues [from (42) to (45) and from (59) to (61)], which surround the aromatic side chain of the conserved Tyr(83) (Beuko-Betts et al., 1985; He et al., 1991). The acidic residues in this area are highly conserved in plant plastocyanins, but in algae plastocyanins some of these residues are replaced by neutral or positively charged amino acids. Remote site electron transfer between plant PCu's and positively charged reaction partners is, therefore, characterized by favorable electrostatic interreactant interactions which lower the activation Gibbs free energy compared with that of the adjacent site. This effect can easily overcome the 50 times less favorable tunnel factor, making the remote site channel overall competitive.

Plastocyanin from the cyanobacterium *Anabaena variabilis* (*A.v.* PCu) deviates from those of other algae and plants in several ways. Primarily, alignment of sequences (Figure 1) shows that while approximately 48 amino acid residues are invariant if only plant plastocyanins are considered, the number is limited to 28 if *A.v.* PCu is included. Second, *A.v.* PCu is among the longest plastocyanins known. Thus, compared to poplar plastocyanin *A.v.* PCu has two additional residues at the N-terminus, one additional residue at the C-terminus, and three additional residues at positions 75−77. Third, *A.v.* PCu has a much higher self-exchange rate constant than other plastocyanins (Dennison et al., 1993). Fourth, at pH ≥ 7 *A.v.* PCu has a positive overall charge of +1 (Aitken, 1975), while other plastocyanins are acidic proteins with a charge of -9 ± 1 (Sykes, 1991). This difference is caused mainly by the absence of negatively charged amino acids at the remote binding site of *A.v.* PCu. The unique charge distribution of *A.v.* PCu indicates that the presence of an acidic patch represents a later evolutionary stage of the plastocyanins (Davis et al., 1980). Finally, kinetic studies have shown that *A.v.* plastocyanin is unlikely to exploit two electron transfer pathways and seems to react only at the adjacent site. This conclusion was based on NMR and inhibition experiments (Jackman et al., 1987b), on ionic strength and pH profiles, and on the use of closely related, variable-charge inorganic reaction partners (Christensen et al., 1992).

These differences make *A.v.* PCu of special interest in the studies of the structure−function relationships of plastocyanins. In particular *A.v.* PCu represents a kind of "natural mutant" on which the lack of negatively charged amino acids at the remote site can be studied. The different electron transfer pattern of *A.v.* PCu compared to other PCu's could, however, reflect not only the different charge distribution but also different structural, conformational, or dynamic features. To disentangle these effects, we have determined the three-dimensional NMR solution structure of *A.v.* PCu and compared the structure with those of other plastocyanins that have been structurally characterized.

Throughout the paper sequence numbers written in parentheses refer to the residues in poplar plastocyanin.

EXPERIMENTAL PROCEDURES

(a) Sample Preparation. A slope of *A. variabilis* (ATCC strain 27892) was kindly supplied by Professor N. G. Carr, University of Warwick. *A.v.* was grown (Jackman et al., 1987b; Christensen et al., 1990b) and plastocyanin was isolated and purified, using the procedure described by Christensen et al. (1990b) after minor modifications. Final purification was performed on an S Sepharose Fast Column to an A_{278}/A_{597} ratio of 1.15:1. The pH was between 6.9 and 7.3 in the NMR samples, and the concentration of the reduced protein was from 1 to 4 mM. Reoxidation was prevented by flushing the solution with nitrogen and sealing the NMR tube under nitrogen. In the initial phase of the

investigation a minor amount (from 1 to 2 mM) of sodium dithionite was added to the samples to maintain the reduction of the copper ion. The samples, however, mostly proved sufficiently stable without this addition.

(b) NMR Experiments. A series of $^1H-^1H$ and $^1H-^{13}C$ chemical shift correlated two-dimensional NMR spectra was recorded at a ^1H frequency of 500 MHz and a ^{13}C frequency of 125.7 MHz on a Bruker AM 500 spectrometer. The ^1H spectra were recorded with a high-sensitivity, dedicated ^1H probe, while the $^1H-^{13}C$ correlated spectra were recorded with an inverse probe, the spectrometer operating in the reverse mode. All spectra were recorded with sequential quadrature detection in the t_2 dimension (Redfield & Kunz, 1975) and time-proportional phase increments (TPPI) in the t_1 dimension (Drobny et al., 1979; Bodenhausen et al., 1980; Marion & Wüthrich, 1983). The temperature was in most cases 298 K although spectra were also recorded at other temperatures in the range from 288 to 305 K.

The $^1H-^1H$ correlated spectra consisted of 1024 t_1 data points and 4096 t_2 data points. A sweep width of 10 000 Hz was used in both dimensions. Three different types of 2D experiments were applied: DQF-COSY (Rance et al., 1983), TOCSY (Braunschweiler & Ernst, 1983; Bax & Davis, 1985), and NOESY (Jeener et al., 1979; Macura et al., 1981). TOCSY spectra were recorded with mixing times of 45 and 52 ms. A DIPSI-2 (Shaka et al., 1988) spin lock pulse of 8.3 kHz was applied in combination with two *z*-filters (Sørensen et al., 1984; Rance, 1987). In the COSY and TOCSY experiments the water signal was suppressed by applying a DANTE pulse sequence (Bodenhausen et al., 1976) during the preparation period. The NOESY spectra were recorded with mixing times of 120 and 160 ms. NOESY spectra in H_2O were acquired with a jump−return read pulse (Plateau et al., 1983; Driscoll et al., 1989) to observe correlations in the fingerprint region that involve α protons otherwise saturated by the water irradiation. In all spectra the residual water resonance was removed by deconvolution before the Fourier transformation (Marion & Bax, 1988). Baseline correction was applied in both frequency dimensions.

A $^1H-^{13}C$ chemical shift correlated HMQC-COSY experiment (Wagner & Brühwiler, 1986) was performed to correlate ^{13}C nuclei with protons on neighboring carbon atoms as well as the directly bound protons. The $^1H-^{13}C$ correlated spectrum was recorded with ^{13}C in natural abundance. The time domain signals consisted of 512 t_1 slices, each with 4096 data points. In both dimensions the sweep width was 10 000 Hz. A radio-frequency field strength of 2.3 kHz was used in the GARP decoupling (Shaka et al., 1985) of ^{13}C during acquisition. Since the decoupler sequence is only efficient within approximately ±4500 Hz of the ^{13}C transmitter frequency, the $^1H-^{13}C$ correlated experiment was run twice, *i.e.*, with the ^{13}C transmitter frequency positioned in the center of the aliphatic region and in the center of the aromatic region, respectively. The lengths of the 90° pulses were 7.5 and 15.9 μs for ^1H and ^{13}C, respectively.

Finally, since overlap in the 2D spectra prevented a complete sequential assignment, a ^1H 3D TOCSY−NOESY spectrum (Vuister et al., 1988; Wijmenga & van Mierlo, 1991) was recorded in H_2O with 256 data points in the t_1 and t_2 dimensions and 1024 data points in the t_3 dimension. The sweep width was 7462 Hz in all three dimensions. The TOCSY part of the experiment was run with a DIPSI-2 spin lock pulse as described for the 2D spectra. The mixing times used were 56 ms for the TOCSY part and 158 ms for the NOESY part of the experiment. Water suppression was achieved by saturation (1 s) during the preparation period and the NOESY mixing time, using a DANTE pulse sequence (Bodenhausen et al., 1976).

Before the data processing the first seven data points in each t_2 slice of the 2D FID, and in each t_2 and each t_3 slice of the 3D FID, were reconstructed routinely by backward linear prediction (Marion & Bax, 1989).

The digital resolution of the $^1H-^1H$ correlated 2D spectra was 2.4 Hz/point in the F_2 dimension and 4.9 Hz/point in the F_1 dimension after zero-filling. The window functions used for resolution enhancement in the NOESY and TOCSY spectra were, in the t_2 dimension, a Gaussian line-broadening function of −15 Hz and a scaling factor of 0.15. A squared sine-bell function with a 70° shift was applied in the t_1 dimension. In the DQF-COSY spectra a sine-bell with a 45° shift and a squared sine-bell with a 90° shift were used along the t_2 dimension, while a squared sine-bell with a 60° shift was applied in the t_1 dimension.

The digital resolution of the 2D $^1H-^{13}C$ correlated spectra was 1.2 Hz/point in the F_2 dimension and 9.8 Hz/point in the F_1 dimension after zero-filling and Fourier transformation. The window functions used in the F_2 dimension of the $^1H-^{13}C$ correlated spectra were a squared sine-bell with a 90° shift and a convolution difference with a line broadening of 15 Hz and a scaling factor of 0.5. A sine-bell shifted 60° and a trapezoidal filter ranging from data point 128 to the end of the FID were used in the F_1 dimension.

Finally, in the 3D spectrum the digital resolution was 7.2 Hz/point in the F_3 dimension and 14.6 Hz/point in both the F_2 and F_1 dimensions after zero-filling to twice the number of data points in these two dimensions. A double parabola window function was used in all three dimensions.

Qualitative discrimination between slow and fast exchanging amide protons was achieved by recording a NOESY spectrum immediately after dissolving the sample in 99.96% D_2O and defining the amide protons still giving rise to cross peaks in the spectrum as slowly exchanging. The recording time was 31 h. In addition, a NOESY spectrum was recorded on a deuterated sample in H_2O over a period of 20 h after solution.

The experimental NMR data were processed on a DEC3000 AXP 400 workstation by locally developed software.

(c) Structural Restraints. Interproton distance restraints were obtained from the NOESY experiments detailed above. The intensities of all NOE cross peaks were determined quantitatively by a combination of linear prediction analysis and simple least squares estimation, as described previously (Gesmar et al., 1994). On the basis of these intensities the NOEs were divided into three classes, “strong”, “medium”, and “weak”. The corresponding upper bound distance restraints were 2.85, 3.56, and 5.00 Å. The distance, 2.85 Å, is the upper bound of the intraresidual αH−NH distances, as given by the covalent structure (Wüthrich et al., 1983). Therefore, the value of the intensity used to separate strong from medium was chosen so that the majority of the intraresidual αH−NH NOEs were classified as strong. Correspondingly, because 3.56 Å is the upper bound for the sequential αH−NH distances, the intensity value used to

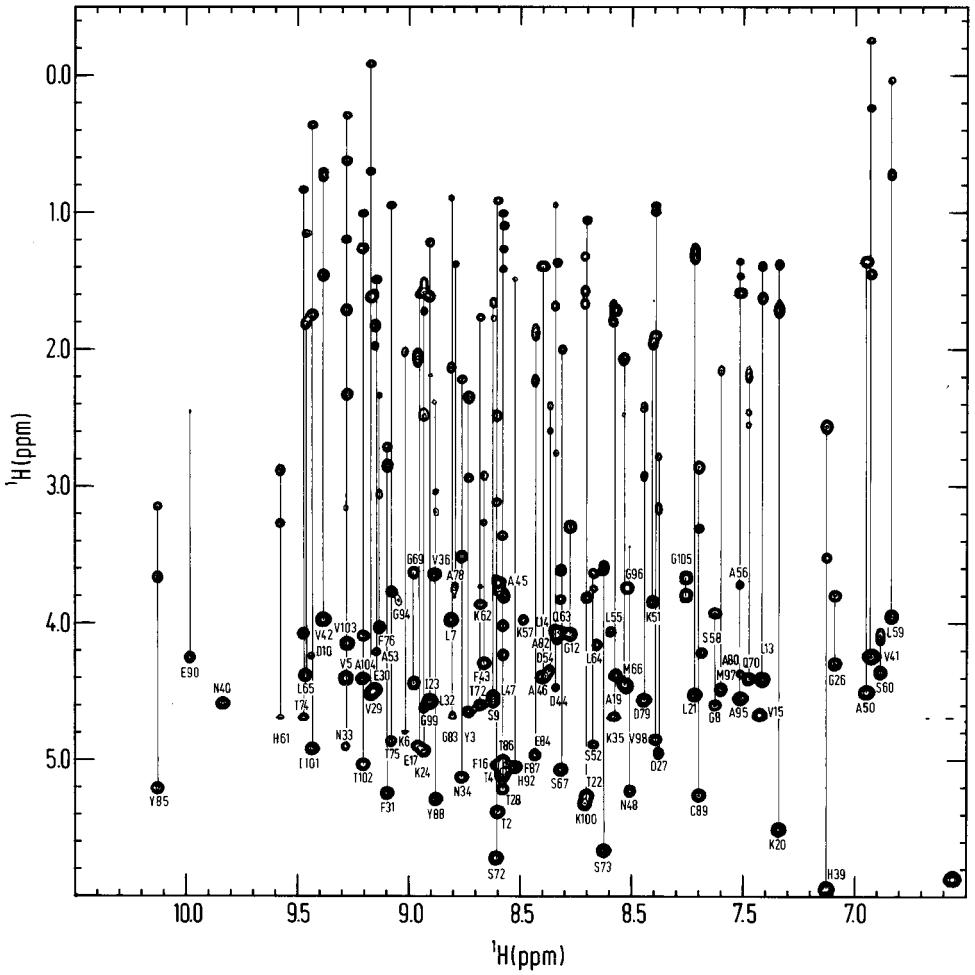

FIGURE 2: Amide proton region of the TOCSY spectrum of *A.v.* plastocyanin in H_2O (2 mM, pH 7.0, 298 K, mixing time 45 ms), showing the correlations between the amide and aliphatic protons.

separate medium from weak was selected in such a way that the sequential αH−NH NOEs that did not fall into the strong class were classified as medium. By this procedure, signals otherwise redundant in the structure determination were used to calibrate the NOE intensities. The upper bound of 5.00 Å, which corresponds to weak, includes a correction of 1.0 Å to account for internal mobility (Braun et al., 1981; Kline et al., 1988). In all cases a lower bound distance restraint of 2.0 Å was applied. Correction factors for pseudoatoms were added to these limits as described by Wüthrich et al. (1983). An additional 0.5 Å was added to the upper limits for distances involving methyl groups (Wagner et al., 1987). Relative scaling of different NOESY spectra was achieved by comparing corresponding signals in the spectra. The classification of the NOEs as strong and medium was done very conservatively by the demand that the intensities exceeded the corresponding separation values by at least three times their individual standard deviation. For a number of weak signals the intensities could not be calculated by the least squares procedure, because of insufficient resolution in the F_1 dimension. These NOEs were classified as weak.

Dihedral angle (ϕ) constraints were derived from the $^3J_{H_\alpha H_N}$ coupling constants obtained from the NOESY spectra by the same linear prediction least squares analysis as used to estimate the NOE cross peak intensities and from the TOCSY and the DQF-COSY spectra by a similar analysis. Backbone ϕ torsion angles were constrained to $-160 < \phi < -80$ for residues with $^3J_{H_\alpha H_N}$ coupling constants exceeding 8 Hz by at least one standard deviation and to $-90 < \phi < -40$ for residues with $^3J_{H_\alpha H_N}$ smaller than 5.5 Hz by one standard deviation.

The two prolines, Pro18 and Pro38, have *cis*-peptide bonds in other plastocyanins (Guss et al., 1986; Moore et al., 1991). Although sequential NOEs indicating neither *cis*- nor *trans*-peptide bonds could be assigned unambiguously, a weak NOE between the Glu17 αH and Pro18 αH, located very close to the diagonal of the spectrum, suggests a *cis*-peptide bond for Pro18. This *cis*-peptide bond is further supported by an NOE between the Glu17 αH and the Ala19 NH, which would be absent in the *trans* conformation for geometrical reasons. For the Pro38 an NOE between the αH and Pro37 αH cannot be observed in the spectra because of a large overlap in this region. However, an NOE between Pro37 βH and His39 NH suggests that this proline also has a *cis*-peptide bond. Therefore, in the structure calculations it was assumed that both of these prolines have *cis*-peptide bonds. It should be noted, however, that structure calculations, carried out with *trans*-peptide bonds for these two prolines, showed no significant changes in the solution structures as compared to those presented here.

The binding site of the copper atom could not be identified in the structures derived from the NMR data. It was, therefore, assumed that the copper atom is bound to the same donor groups as in other plastocyanins, that is, δN of His39-(37) and His92(87), γS of Cys89(84), and δS of Met97(92) (Colman et al., 1978; Guss et al., 1986; Moore et al., 1988a,

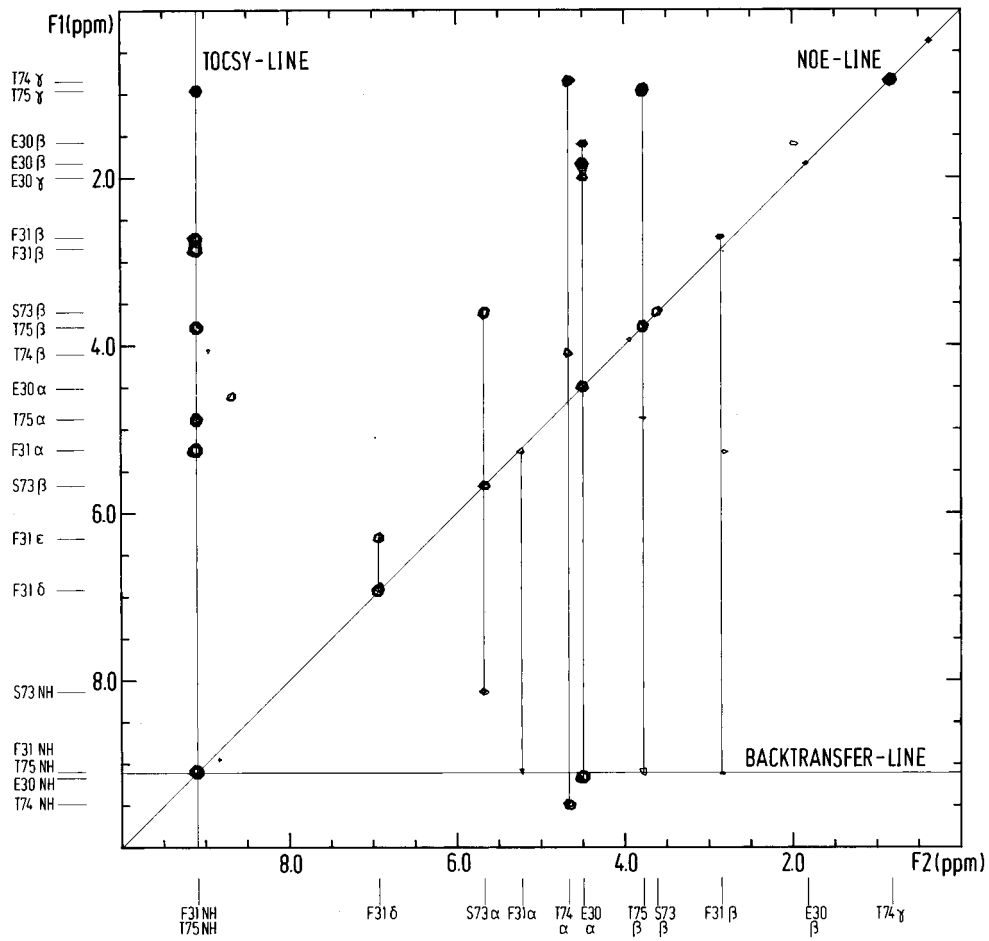

FIGURE 3: The F_1,F_2 plane of the 3D ^{1}H TOCSY−NOESY spectrum of *A.v.* plastocyanin at $F_3 = 9.12$ ppm, corresponding to the resonance frequency of the amide proton of Phe31 (and of Thr75). NOE connectivities from the amide protons of Phe31 and Thr75 are seen on the diagonal. The TOCSY patterns of the spin systems, from which the NOE connectivities are derived, are observed along F_1.

1991; Redinbo et al., 1993; Bagby et al., 1994). Accordingly, the copper atom was introduced in the structure calculation as an independent segment and placed in the apo molecule by a series of copper−ligand distance restraints similar to the NOE-derived ^{1}H−^{1}H distance restraints. These restraints are Cu−δN His39 (2.16 ± 0.2 Å), Cu−γS Cys89 (2.15 ± 0.2 Å), Cu−δN His92 (2.37 ± 0.2 Å), and Cu−δS Met97 (2.88 ± 0.2 Å). To obtain the correct geometry of the copper atom, ligand−copper angles were also incorporated in the calculations to ensure coplanarity with the imidazole rings and an overall geometry around the copper atom that is approximately tetrahedral. The angles incorporated were X−Cu−X angles (X = S or N) with an equilibrium value of 110° and a force constant of 10 kcal·mol^{-1}·rad^{-2}, Cu−N−C angles with an equilibrium value of 127° and a force constant of 50 kcal·mol^{-1}·rad^{-2}, and Cu−S−C angles with an equilibrium value of 120° and a force constant of 50 kcal·mol^{-1}·rad^{-2} (Moore et al., 1991).

(d) Structure Calculations. The calculation of the structures and the assignment of the NOE correlations were carried out as an iterative process. The structure calculations were carried out using the program X-PLOR (Brünger, 1992). The starting point was generation of substructures, using the DG-SUB-EMBED protocol. The substructures included the backbone nitrogen, carbon, and hydrogen atoms and the β- and γ-carbons. Subsequently, distance geometry simulated annealing (DGSA) calculations (Nilges et al., 1988) were carried out. The structures were first run through 200 cycles of restrained energy minimization and then subjected to 4 ps restrained molecular Verlet dynamics at a temperature of 3000 K. This step was followed by an 8 ps cooling to 300 K. The time steps were 0.001 ps. The temperature was varied in steps of 50 K during the cooling stage. The van der Waals energy function was represented by the simple repel function during the initial restrained energy minimization, the restrained molecular dynamics, and the cooling stage. During the cooling stage the van der Waals interactions were increased by varying the force constant of the van der Waals repel function from 0.003 to 4 kcal·mol^{-1}·Å^{-4}.

Finally, the structures from the DGSA procedure were run through 3000 cycles of restrained energy minimization. In this final refinement the full CHARMM energy function (Brooks et al., 1983) was employed, including a Lennard-Jones potential function and an explicit hydrogen bond energy term. During all calculations the force constants used for the NOE and torsion angle restraints were 50 kcal·mol^{-1}·Å^{-2} and 200 kcal·mol^{-1}·rad^{-2}, respectively.

Structures were visualized on a Silicon graphics workstation using the program Insight II (Biosym Technology, San Diego, CA).

RESULTS

(a) Sequential Assignments. An essentially complete assignment of the ^{1}H resonances was achieved by well-established procedures (Wüthrich, 1986). The quality of the spectra used in the assignment is illustrated in Figure 2. The alanines, threonines, and almost all of the valines were

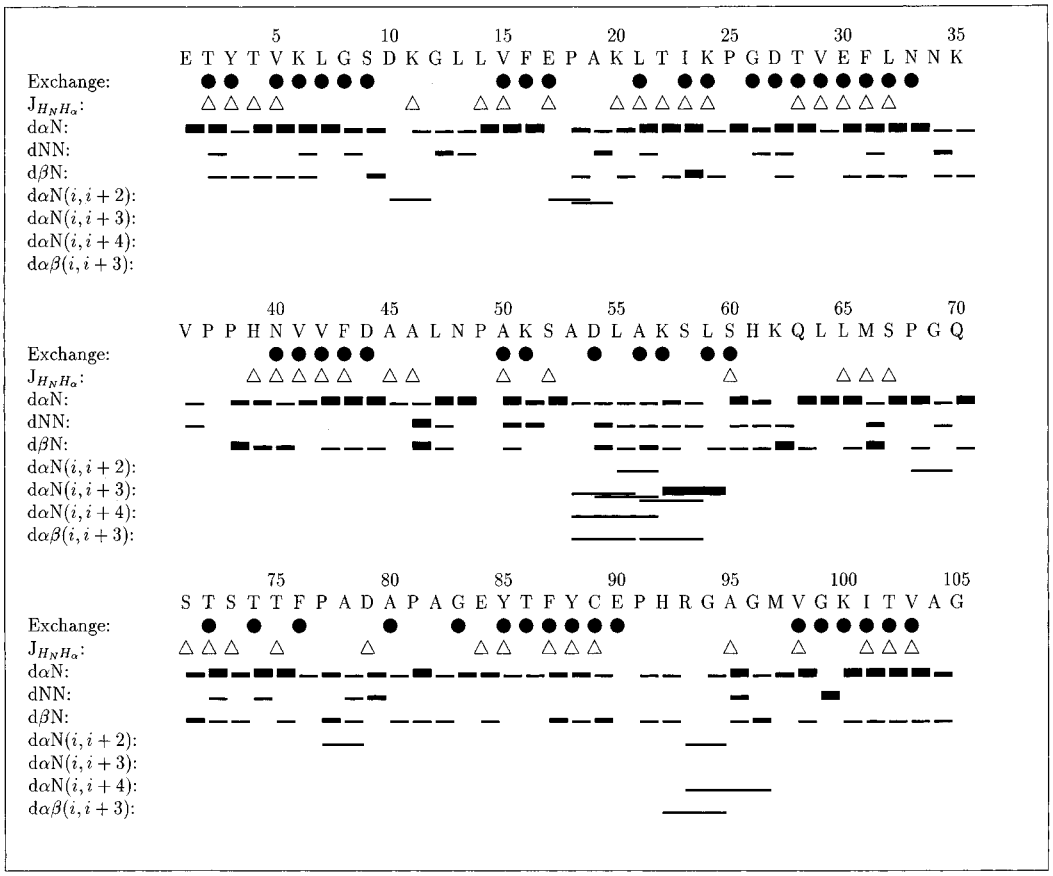

FIGURE 4: Sequential and medium-range NOE connectivities in *A.v.* plastocyanin. For Pro residues the connectivities to the δ protons are shown. The intensity of the NOE connectivities is indicated by the thickness of the bars. Backbone amide protons exchanging slowly with deuterons in D_2O are indicated with filled circles (●). Triangles (△) indicate $J_{H_NH_\alpha}$ coupling constants that exceed 8 Hz by at least one standard deviation.

identified from their unique spin systems. Among the glycines only Gly 105 was identified from the unique glycine pattern of two cross peaks in the fingerprint region of the DQF-COSY spectrum. The other glycines were identified from the cross peaks in the TOCSY and $^1H-^{13}C$ HMQC-COSY spectra. The $^1H-^{13}C$ HMQC spectrum was valuable in the assignment of spin systems due to the large dispersion in the ^{13}C dimension. In particular, a comparison of the ^{13}C chemical shifts with the random coil ^{13}C values was useful in the assignment process. Most aromatic amino acids could be identified on the basis of the strong NOEs between the β protons and the δ protons. Also the asparagines could be identified from the NOEs between the β protons and the amine protons. Several amino acids were not identified until the sequential assignment due to overlap, degenerated resonances, or ring current shifts. Ring current shifts were observed for the β protons of Leu7 and Phe87 and the α proton of Gly99.

Sequential assignments were made on the basis of a series of 2D NOESY spectra and a 3D ^1H TOCSY−NOESY spectrum. The 2D NOESY spectra were recorded at different temperatures, to allow discrimination of overlapping NH frequencies. In addition to NOE connectivities the 3D ^1H TOCSY−NOESY spectrum shows TOCSY patterns from the involved protons which make it possible to assign NOEs in areas with overlap in the amide and α proton regions. This is illustrated in Figure 3, which shows an F_1F_2 slice at an F_3 frequency corresponding to the resonance of the amide proton of Phe31. Further, the 3D spectrum allowed the identification of the nine prolines of *A.v.* PCu. All sequential NOEs are indicated in Figure 4.

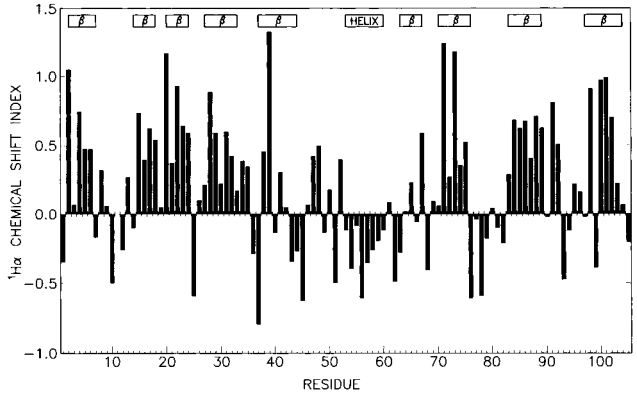

FIGURE 5: Plot of the difference between the $^1H_\alpha$ chemical shifts of *A.v.* plastocyanin and random coil values (Wishart & Sykes, 1994, Table IX) as function of residue number. For the glycines the average of the chemical shifts of the two α protons was used. The actual secondary structures, as determined through NOE connectivities and amide hydrogen exchange rates, are indicated above the graph. A grouping of four or more residues with deviations from random coil $^1H_\alpha$ chemical shifts of less than −0.10 ppm suggests a helix, while a grouping of three or more residues with deviations from random coil $^1H_\alpha$ chemical shifts larger than 0.10 ppm indicates a β-strand (Wishart & Sykes, 1994). All other regions are designated as coil.

(b) Secondary Structure. The NMR data summarized in Figure 4 indicate that β-sheets are the principal secondary structure elements in *A.v.* PCu. Thus, numerous intense $d_{\alpha N}$ connectivities, a series of $^3J_{H_\alpha H_N}$ coupling constants ≥8 Hz,

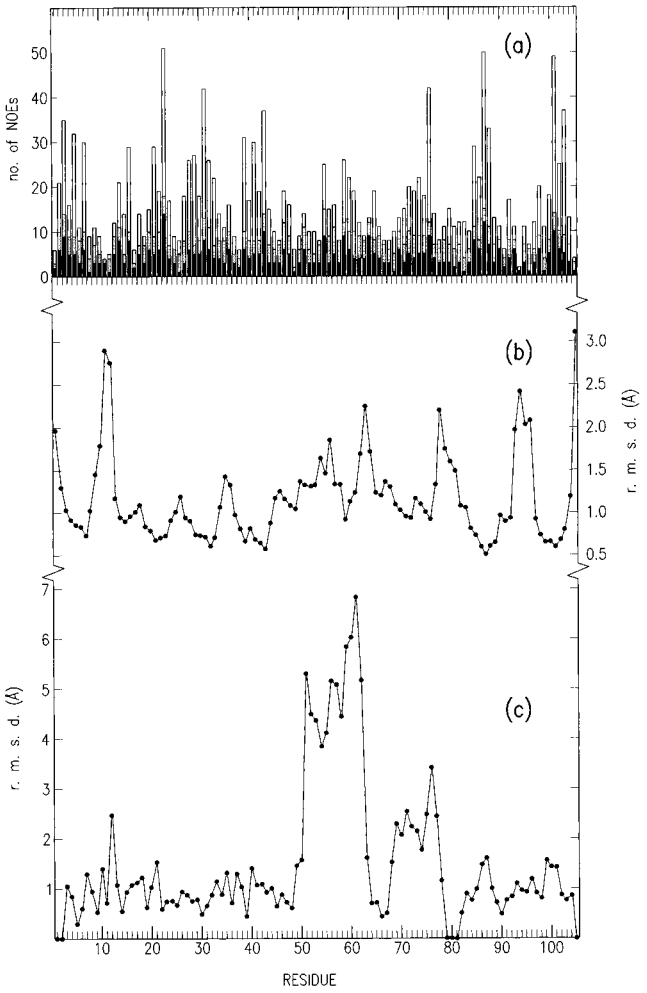

FIGURE 6: (a) Distribution of the NOE connectivities used in the structure calculation of *A.v.* plastocyanin. All sequential and interresidual NOE connectivities are represented twice, once for each of the involved protons. (b) Average N, C′, and C_α backbone rms deviations (Å) from the mean structure for the 20 solution structures of *A.v.* plastocyanin with the lowest total energy. (c) N, C′, and C_α backbone rms deviations (Å) between the average *A.v.* and poplar plastocyanins. The extra amino acid residues in *A.v.* (Glu1−Thr2, Pro77−Asp79, and Gly105) relative to poplar plastocyanin are excluded from the superposition. However, these residues are included in the figure with rms deviations set to zero, to maintain the numbering of the residues.

and the corresponding patterns of slowly exchanging amide hydrogens are all in accordance with β-sheets. In the region from Ala53 to Ser60 a helix is indicated by a series of $d_{\alpha N}(i,i+2)$, $d_{\alpha N}(i,i+3)$, $d_{\alpha N}(i,i+4)$, and $d_{\alpha\beta}(i,i+3)$ connectivities and small $^3J_{H_\alpha H_N}$ coupling constants. Also a series of slowly exchanging amide hydrogens indicates the presence of a helix in this region.

A further indication of the type of secondary structure present can be obtained from the pattern of the $^1H_\alpha$ chemical shifts (Wishart & Sykes, 1994). Thus, the plot in Figure 5 confirms that β-strands are the dominant secondary structure elements, while the only helix in the protein, from Ala53 to Ser60, is clearly indicated by the pattern of $^1H_\alpha$ chemical shifts in this region.

(c) Quality of the Calculated Structures. A total of 1137 NOE distance restraints were obtained from the NOESY spectra and were used in the final structure calculations. These restraints are 474 intraresidual restraints, 189 sequential restraints, and 474 interresidual restraints. Furthermore,

FIGURE 7: Superposition of 18 of the 20 selected solution structures of *A.v.* plastocyanin with the lowest total energy. Only the C′, C_α, and N backbone atoms for the β-sheet regions are superimposed. These regions included the residues from Thr2 to Leu7, Leu14 to Pro18, Lys20 to Lys24, Asp27 to Arg33, Pro37 to Asp44, Glu70 to Pro76, Gly83 to Cys89, and Met97 to Ala104.

Table 1: Average rms Deviations (Å) between the 20 Selected Structures and the Mean Structure of *A. variabilis* Plastocyanin

all atoms[a]	backbone[a]	all β-sheet atoms[b]	β-sheet backbone[b]
1.75	1.25	1.25	0.76

[a] Fitting was done on all heavy atoms and on all N, C_α, and C′ backbone atoms, respectively. [b] Fitting was done on all heavy atoms and on all N, C_α, and C′ backbone atoms from the β-sheet region, respectively. The β-sheet region included the residues from Thr2 to Leu7, Leu14 to Pro18, Lys20 to Lys24, Asp27 to Asn33, Pro37 to Asp44, Gln70 to Phe76, Gly83 to Cys89, and Met97 to Ala104.

46 dihedral angle restrains and 4 distance restraints involving the copper atom were included in the structure calculations. The distribution of NOEs is shown in Figure 6a.

A total of 60 structures were calculated. A best-fit superposition of the backbone of 18 of the 20 structures with the lowest total energy is shown in Figure 7. The remaining two structures have a poorly defined helix. No NOE violations larger than 0.35 Å were observed in any of the 20 structures. The distances and restraints between the copper and the four ligand atoms [δN of His92(87) and His39(37), γS of Cys89(84), and δS of Met97(92); see Experimental Procedures] are all consistent with the NOE-derived distance restraints. Thus, only three distance violations (0.010, 0.011, and 0.039 Å) involving the copper atom were observed in the 20 selected structures. The observation of the proton resonance of ϵNH of His39(37) further supports the binding of Cu to the δN atom of this histidine. Average values of the rms deviations of the 20 structures from the mean structure are given in Table 1. In Figure 6b are shown the average residual rms deviations from the mean structure.

The good agreement between the calculated structures and the experimental data is further emphasized by the statistics in Table 2. Thus, the average rmsd from the distance restraints is 0.017 Å, and the deviations from the ideal bond lengths, angles, and improper torsion angles used in X-PLOR are 0.0144 Å, 3.313°, and 0.435°, respectively. Finally, the Lennard-Jones van der Waals energy has a negative value

Table 2: Structural Statistics

	mean	range
rms Deviations from NOE Restraints and from the Idealized Geometry Used within X-PLOR		
NOE (Å)	0.017	0.006
bond length (Å)	0.0144	0.0017
bond angles (deg)	3.313	0.279
improper dihedral angles (deg)	0.435	0.125
X-PLOR Potential Energies (kcal·mol^{-1})[a]		
total	−1297.465	289.848
van der Waals	−414.958	36.003
NOE restraints	16.676	12.200
dihedral angle restraints	1.921	6.209

[a] The force constants of the NOE and torsion angle terms were 50 kcal·mol^{-1}. Å^{-2} and 200 kcal·mol^{-1}·rad^{-2}, respectively.

of −414.958 kcal·mol^{-1}, which indicates that the structures have good nonbonding contacts. The average structure of *A.v.* PCu is shown in Figure 8.

(d) Hydrogen Bonds. The obtained structure of *A.v.* PCu is characterized by numerous hydrogen bonds. Thus, 50 slowly exchanging amide protons have been observed. Among these, a total of 38 amide protons are involved in hydrogen bonds within the β-sheets or the helical region. The remaining 12, which are the amide protons of Gly8(6), Ser9(7), Val15(13), Lys24(22), Gly26(24), Asp27(25), Ala50(48), Lys51(49), Asp54(52), Ala80(78), Thr86(81), and Glu90 (85), are involved in hydrogen bonds associated either with turns or with the tertiary structure of the protein.

Among the hydrogen bonds associated with turns and the tertiary structure six can be identified immediately from the calculated structures. These are Ser9(7) NH···OC Leu13-(11), Val15(13) NH···OC Leu13(11), Gly26(24) NH···OC Lys24(22), Lys51(49) NH···OC Pro49(47), Asp54(52) NH···γOC Asp54(52), and Glu90(85) NH···OC Tyr88(83). In 10 or more of the selected structures these hydrogen bonds are characterized by the geometry necessary for establishing a hydrogen bond, that is, a distance <3.5 Å between the N and O atoms and a N−H−O bond angle in the range from 120° to 180° (Baker & Hubbard, 1984). The remaining six amide protons are involved in hydrogen bonds in five to nine of the selected structures. These hydrogen bonds are the following: Gly8(6) NH···OC Val15(13), Lys24(22)NH···γOC Asp27(25), Asp27(25) NH···OC Lys24(22), Ala50(48) NH···γOC Asn48(46), Thr86(81) NH···OC Leu47(45), and Ala80(75) NH···OC Pro77(72).

Furthermore, the side chain hydrogen bonds Ser60(58) γOH···OC Lys57(55), Tyr85(80) ηOH···OC Pro81(76), and His39(37) ϵNH···OC Lys35(33) were observed in 9, 12, and 15 structures, respectively. These hydrogen bonds are all supported by the observation of the corresponding OH and NH proton resonances in the NMR spectra, which indicates decreased exchange rates of these protons.

Finally, according to the definition above, the six hydrogen bonds His39(37) NH···OC Leu65(63), Asn48(46) NH···-OC Ala46(44), His61(59) NH···OC Val41(39), Gly69(67) NH···OC Asn33(31), His92(87) NH···OC Cys89(84), and Gln70(68) NH···OC Ser67(65) were observed in nine or more of the selected structures, even though the amide protons were not characterized as slowly exchanging. Also, three hydrogen bonds between side chain atoms and backbone atoms, found in other plastocyanins, are observed in a few (three to five) of the selected structures. These three hydrogen bonds are Asn33(31) δNH$_2$···OC Leu65(63), Asn33(31) δNH$_2$···OC Ser67(65), and Asn34(32) δNH$_2$···-OC Gly8(6).

DISCUSSION

(a) Description of the Structure. Despite the low homology and the longer peptide chain, the global fold of *A.v.* PCu is very similar to those of other plastocyanins (Colman et al., 1978; Moore et al., 1991; Bagby et al., 1994). Thus, as sketched in Figure 9, the structure of *A.v.* PCu consists of two β-sheets (I and II), containing eight β-strands which fold up in a barrel with a hydrophobic core. The barrel has two ends made up by turns and loops that connect the β-strands. Sheet I contains four β-strands formed by the residues from Thr2 to Leu7(5), Leu14(12) to Pro18(16), Asp27(25) to Asn33(31), and Gln70(68) to Phe76(74). Sheet II also contains four β-strands formed by the residues from Lys20(18) to Lys24(22), Pro37(35) to Asp44(42), Gly83-(78) to Cys89(84), and Met97(92) to Ala104(99). In the selected structures all β-strands were characterized by a ϕ dihedral angle in the range from −180° to −60° and a ψ dihedral angle in the range from 20° to 180°.

The helix from Ala53(51) to Ser60(58) is longer and more regular than in other structurally characterized plastocyanins. Thus, four helical hydrogen bonds are observed in the majority of the selected structures. These hydrogen bonds are Lys57(55) NH···OC Ala53(51), Ser58(56) NH···OC Asp54(52), Leu59(57) NH···OC Leu55(53), and Ser60(58) NH···OC Ala56(54), all of which indicate an α-helix in this region. However, 3_{10}-helical hydrogen bonds to Ser58(56), Leu59(57), and Ser60(58) are also observed in some of the structures. The helix is further stabilized by a hydrogen bond between the side chain γOH atom of Ser60(58) and the Lys57(55) backbone O atom, which is observed in one-half of the selected structures. Finally, 2 of the 20 selected structures have a poorly defined helix. This observation, together with the pattern of helical hydrogen bonding just mentioned and the pattern of slowly and fast exchanging amide hydrogens (Figure 4), indicates a relatively flexible helical region. Further evaluation of the mobility of the molecule based on relaxation studies is in progress.

Finally, the helix is followed by a short β-strand from Gln63(61) to Ser67(65), also observed in other plastocyanins (Bagby et al., 1994; Guss et al., 1986).

The extra residues found in *A.v.* PCu as compared with other plastocyanins (Figure 1) do not have any major influence on the structure. Thus, at the N- and C-terminal ends of the polypeptide chain the extra residues form a natural extension of the β-strands. The extra residues from residue 77 to residue 79 make a loop in the "south" end of the molecule, opposite the active sites (Figures 9 and 10). Although this region is less well-defined, the calculated structures indicate a β-turn from Pro77 to Ala80(75). Thus, in five of the selected structures the hydrogen bond Ala80-(75) NH···OC Pro77 is established. This hydrogen bond is supported by the slow exchange of the Ala80(75) amide hydrogen. As in other plastocyanins (Moore et al., 1991; Bagby et al., 1994) the Cu atom is bound to δN of His92-(87) and His39(37), γS of Cys89(84), and δS of Met97(92) (see Results).

(b) Comparison of A.v. PCu and Other Plastocyanins. As noted, *A.v.* PCu has a series of structural features in common

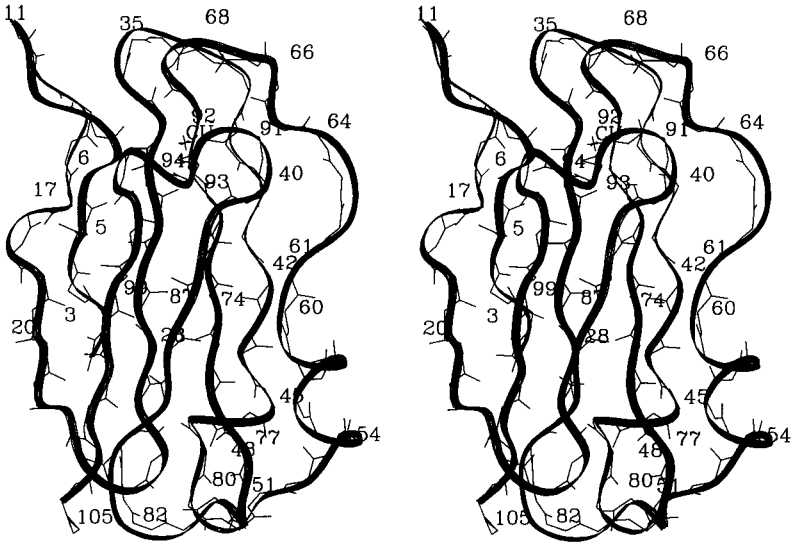

FIGURE 8: Average solution structure of *A.v.* plastocyanin. Only backbone atoms are shown.

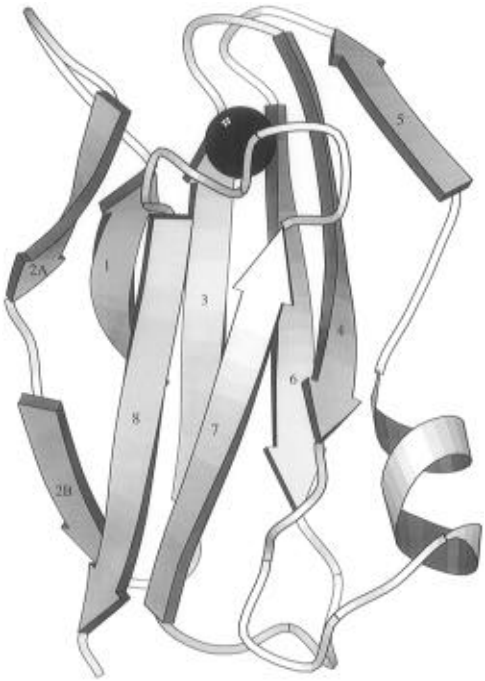

FIGURE 9: Schematic representation of the structure of *A.v.* plastocyanin. Labels indicate the β-strand numbers. The figure was prepared using the program MOLSCRIPT (Kraulis, 1991).

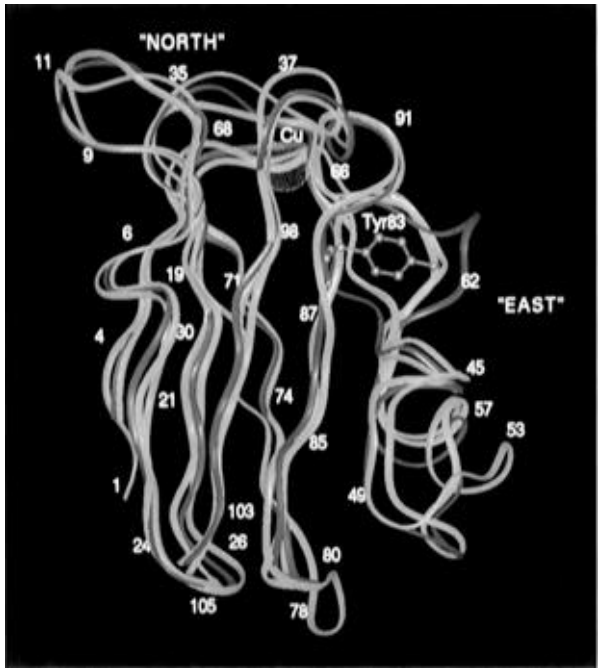

FIGURE 10: Comparison between the average solution structures of *A.v.* plastocyanin (yellow color) and parsley plastocyanin (blue color) and the crystal structure of poplar plastocyanin (purple color). Only the backbone atoms are superimposed. The extra amino acid residues in *A.v.* relative to the other two plastocyanins were excluded from this superposition. Only backbone atoms are shown. The Tyr residue (located in position 83 in poplar plastocyanin), which seems important for the electron transfer, is also shown.

with other structurally characterized plastocyanins, despite the differences in primary structure and charge. These features include the pattern of the β-sheets and the hydrogen bonds within the β-sheets, which results in a close similarity in the overall fold. Also the ring current shifted protons of residues Gly99(94), Leu7(5), and Phe87(82) observed in *A.v.* PCu are shared with other NMR-characterized plastocyanins (Driscoll et al., 1987; Chazin & Wright, 1988; Moore et al., 1988b, Bagby et al., 1994) and indicate similar environments for these amino acid residues in the different plastocyanins. This is confirmed by the structure obtained here for *A.v.* PCu. Further, the experimental data indicate that the two conserved prolines, Pro18(16) and Pro38(36), have *cis*-peptide bonds. Such bonds have also been found for Pro(16) and Pro(36) in poplar and French bean plastocyanins (Guss et al., 1986; Moore et al., 1991).

Several of the hydrogen bonds outside the β-sheet region are also found in other plastocyanins, which supports the structural similarity with these. This holds for the following hydrogen bonds: Ser9(7) NH···OC Leu13(11), Asn33(31) δNH_2···OC Leu65(63), Asn33(31) δNH_2···OC Ser67(65), Asn34(32) δNH_2···OC Gly8(6), His39(37) ϵNH···OC Lys35-(33), Gly69(67) NH···OC Asn33(31), Gln70(68) NH···OC Ser67(65), Tyr85(80) ηOH···OC Pro81(76), Thr86(81) NH···-OC Leu47(45), and His92(87) NH···OC Cys89(84).

The most striking deviation of the *A.v.* PCu structure from the structures of higher plant plastocyanins is the difference in the local structures of the polypeptide chains on the east side. As shown in Figure 6c, this difference is well beyond the uncertainty of the obtained *A.v.* PCu structure. Primarily,

the β-turn formed by residues (58) to (61) in plant plastocyanins is absent in *A.v.* PCu (Figure 10). This is also seen in plastocyanins where residues (57) and (58) are deleted, as, for example, in green algae plastocyanins. Thus, *A.v.* PCu resembles green algae plastocyanins even though *A.v.* PCu does have the residues (57) and (58) (Figure 10). Secondly, the absence in *A.v.* PCu of the turn from residues (58) to (61) results in a displacement of the polypeptide chain on the east side, whereby residue Ser60(58) in *A.v.* PCu obtains a position similar to that of the conserved Ser(56) in other plastocyanins. In accordance with this displacement the γOH proton of Ser60(58) forms a hydrogen bond to the CO group of Lys57(55), in the same way as the γOH proton of Ser(56) forms a hydrogen bond to residue (52) in other plastocyanins (Moore et al., 1991; Bagby et al., 1994). In all of these cases the hydrogen bonds are supported by the observation of the OH resonances in the proton NMR spectra, indicating decreased exchange rates of these protons.

The displacement of the peptide chain, caused by the absence of the turn from residue (58) to residue (61), is compensated for by an extension of the N-terminal end of the helix, as compared to other plastocyanins. Thus, in *A.v.* PCu the helix extends from Ala53(51) to Ser60(58), forming a complete two-turn helix. In contrast, the helix only includes the residues from (51) to (56) in Frensh bean plastocyanin (Moore et al., 1991) and the residues from (52) to (56) in parsley and poplar plastocyanins (Bagby et al., 1994; Guss et al., 1986), corresponding to only about one and a half turn. As a consequence of the extension of the helix, *A.v.* PCu retains, in general, the same tertiary folding of the peptide chain, as found in other plastocyanins. An exception from this similarity is a slight displacement of the β-strand from Gln70 to Phe76, as indicated in Figures 6c and 10. Also, as noted, the extra residues from 77 to 79 result in the additional β-turn from Pro77 to Ala80.

The structural differences and similarities between *A.v.* PCu and other plastocyanins just discussed offer a clue to the different electron transfer reactivity patterns. As noted, unlike other plastocyanins, most kinetic data for *A.v.* PCu suggest that electron transfer is dominated entirely by the adjacent site (Jackman et al., 1987b; Christensen et al., 1992). The reason for the insignificant reactivity at the remote site in *A.v.* PCu can most straightforwardly be ascribed either to the absence of negatively charged amino acid residues near this site or to structural differences as compared to other plastocyanins. As noted, the largest structural difference between *A.v.* PCu and higher plant plastocyanins is the absence of the (58)−(61) β-turn at the remote site. However, other plastocyanins that also lack this turn still show considerable remote site reactivity (Bagby et al., 1994). It seems, therefore, unlikely that structural changes should be the main reason for the insignificant or absent electron transfer reactivity of *A.v.* PCu at the remote site.

More likely the insignificant electron transfer reactivity of the remote site of *A.v.* PCu is caused by the large reduction of the negative charge at this site as compared with other plastocyanins. Thus, in plastocyanin from algae, parsley, and other species, where the β-turn from (58) to (61) is also absent, the negative charge at the remote site has been retained through the introduction of other negatively charged amino acids at this site. This is illustrated in Figure 11. Poplar PCu has six negative charges at this location, namely, Asp(42), Glu(43), Asp(44) and Glu(59), Glu(60), Asp(61),

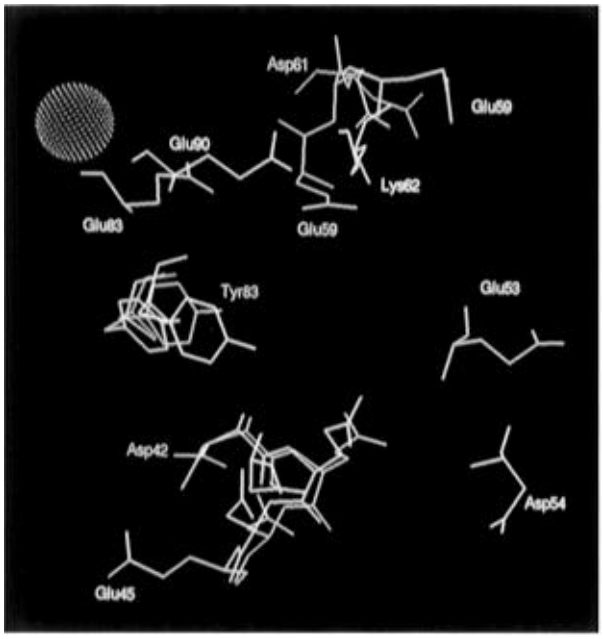

FIGURE 11: Negatively charged amino acids located at the remote site of *A.v.* plastocyanin (yellow color), parsley plastocyanin (blue color), and poplar plastocyanin (purple color). The following amino acids are indicated: for poplar plastocyanin, Asp42−Asp44, Glu59−Asp61, and Tyr83; for parsley plastocyanin, Asp42−Glu45, Glu53, Glu59, Tyr81(83), and Glu83(85); and for *A.v.* plastocyanin, Asp44(42), Asp54(52), Tyr88(83), and Glu90(85).

while parsley has seven, Asp42(42), Glu43(43), Asp44(44), Glu45(45) and Glu53(53), Glu57(61), and Glu83(85). In comparison, *A.v.* Pcu has only the negatively charged residues Asp44(42), Asp54(52), and Glu90 (85) near the remote site. Moreover, the charge from these residues is partly neutralized by the positively charged Lys62(60) and by the positively charged His61(59) at pH $\leq$7. Consequently, the negative charge near the remote site of *A.v.* PCu is strongly reduced in comparison with other plastocyanins. This makes the remote site in *A.v.* PCu much less attractive for an electrostatic interaction with cytochrome *f* and positively charged inorganic reaction partners. Furthermore, electrostatic attraction is a crucial prerequisite for electron transfer reactivity at the remote site. This holds since the associated interreactant interaction provides the lowering of the activation free energy necessary to compensate for the less attractive long-range tunneling through the protein as compared with the adjacent site (Christensen et al., 1990a). It, therefore, seems most likely that the lack of negatively charged residues rather than specific structural features of *A.v* PCu is the main reason for the failure of the remote site of this plastocyanin to function as a significant electron transfer site.

ACKNOWLEDGMENT

We are most grateful to Professor N. G. Carr and Dr. J. Scanlan at the University of Warwick for the donation of several cultures of *A. variabilis*. We thank Dr. Georg Ole Sørensen for computational assistance and Dr. Søren M. Kristensen and Mr. Morten Dahl Sørensen for technical assistance during the recording of the spectra.

SUPPORTING INFORMATION AVAILABLE

Tables containing ^{1}H chemical shifts of *A. variabilis* plastocyanin and distance and dihedral angle restraints used

in the structure calculations (31 pages). Ordering information is given on any current masthead page.

REFERENCES

Aitken, A. (1975) *Biochem. J. 149*, 675−683.

Bagby, S., Driscoll, P. C., Goodall, K. G., Redfield, C., & Hill, H. A. O. (1990) *Eur. J. Biochem. 188*, 413−420.

Bagby, S., Driscoll, P. C., Harvey, T. S., & Hill, H. A. O. (1994) *Biochemistry 33*, 6611−6622.

Baker, E. N., & Hubbard, R. E. (1984) *Prog. Biophys. Mol. Biol. 44*, 97−179.

Bax, A., & Davis, D. G. (1985) *J. Magn. Reson. 65*, 355−360.

Beuko-Betts, D., Chapman, S. K., Knox, V., & Sykes, A. G. (1985) *Inorg. Chem. 24*, 1677−1681.

Bodenhausen, G., Freeman, R., & Morris, G. A. (1976) *J. Magn. Reson. 23*, 171−175.

Bodenhausen, G., Vold, R. L., & Vold, R. R. (1980) *J. Magn. Reson. 37*, 93−106.

Boulter, D., Haslett, B. G., Peacock, D., Ramshaw, J. A. M., & Scawen, M. D. (1977) in *Plant Biochemistry II. International Review of Biochemistry* (Northcote, D. H., Ed.) Vol. 13, pp 1−40, University Park Press, Baltimore, MD.

Braun, W., Brösch, C., Brown, L. R., Gõ, N., & Wüthrich, K. (1981) *Biochim. Biophys. Acta 667*, 377−396.

Braunschweiler, L., & Ernst, R. R. (1983) *J. Magn. Reson. 53*, 521−528.

Brooks, B., Bruccoleri, R., Olafson, B., States, D., Swaminathan, S., & Karplus, M. (1983) *J. Comput. Chem. 4*, 187−217.

Brünger, A. T. (1992) *X-PLOR Manual*, Yale University, New Haven, CT.

Chazin, W. J., & Wright, P. E. (1988) *J. Mol. Biol. 202*, 623−636.

Christensen, H. E. M., Conrad, L. S., Mikkelsen, K. V., Nielsen, M. K., & Ulstrup, J. (1990a) *Inorg. Chem. 29*, 2808−2816.

Christensen, H. E. M., Conrad, L. S., & Ulstrup, J. (1990b) *Photosynth. Res. 25*, 73−76.

Christensen, H. E. M., Ulstrup, J., & Sykes, A. G. (1990c) *Biochim. Biophys. Acta 1039*, 94−102.

Christensen, H. E. M., Conrad, L. S., & Ulstrup, J. (1992) *Acta Chem. Scand.*, 508−514.

Collyer, C. A., Guss, J. M., Sigimura, Y., Yoshizaki, F., & Freeman, H. C. (1990) *J. Mol. Biol. 211*, 617−632.

Colman, P. M., Freeman, H. C., Guss, J. M., Murata, M., Norris, V. A., Ramshaw, J. A. M., & Venkatappa, M. P. (1978) *Nature (London) 272*, 319−324.

Davis, D. J., Krogmann, D. W., & San Pietro, A. (1980) *Plant Physiol. 65*, 697−702.

Dennison, C., Kyritsis, P., McFarlane, W., & Sykes, A. G. (1993) *J. Chem. Soc., Dalton Trans.*, 1959−1963.

Driscoll, P. C., Hill, H. A. O., & Redfield, C. (1987) *Eur. J. Biochem. 170*, 279−292.

Driscoll, P. C., Clore, M. G., Beress, L., & Gronenborn, A. M. (1989) *Biochemistry 28*, 2178−2187.

Drobny, G., Pines, A., Sinton, S., Weitekamp, D. P., & Wemmer, D. (1979) *Faraday Div. Chem. Soc. Symp. 13*, 49−55.

Gesmar, H., Nielsen, P. F., & Led, J. J. (1994) *J. Magn. Reson. B103*, 10−18.

Gross, E. L. (1993) *Photosynth. Res. 37*, 103−116.

Guss, J. M., & Freeman, H. C. (1983) *J. Mol. Biol. 169*, 521−563.

Guss, J. M., Harrowell, P. R., Murata, M., Norris, V. A., & Freeman, H. C. (1986) *J. Mol. Biol. 192*, 361−387.

Haehnel, W. (1984) *Annu. Rev. Plant Physiol. 35*, 659−693.

He, S., Modi, S., Bendall, D. S., & Gray, J. C. (1991) *EMBO J. 10*, 4011−4016.

Jackman, M. P., McGinnis, J., Sykes, A. G., Collyer, C. A., Murata, M., & Freeman, H. C. (1987a) *J. Chem. Soc., Dalton Trans.*, 2573−2577.

Jackman, M. P., Sinclair-Day, J. D., Sisley, M. J., Sykes, A. G., Denys, L. A., & Wright, P. E. (1987b) *J. Am. Chem. Soc. 109*, 6443−6449.

Jeener, J., Meier, B. H., Bachmann, P., & Ernst, R. R. (1979) *J. Chem. Phys. 71*, 4546−4553.

Kline, A. D., Braun, W., & Wüthrich, K. (1988) *J. Mol. Biol. 204*, 675−724.

Kraulis, P. J. (1991) *J. Appl. Crystallogr. 24*, 946−950.

Macura, S., Huang, Y., Suter, D., & Ernst, R. R. (1981) *J. Magn. Reson. 43*, 259−281.

Malkin, R., & Malmström, B. G. (1970) *Adv. Enzymol. 33*, 177−244.

Marion, D., & Bax, A. (1988) *J. Magn. Reson. 79*, 352−356.

Marion, D., & Bax, A. (1989) *J. Magn. Reson. 83*, 205−211.

Marion, D., & Wüthrich, K. (1983) *Biochem. Biophys. Res. Commun. 113*, 967−974.

McGinnis, J., Sinclair-Day, J. D., & Sykes, A. G. (1986) *J. Chem. Soc., Dalton Trans.*, 2007−2009.

McGinnis, J., Sinclair-Day, J. D., Sykes, A. G., Powls, R., Moore, J., & Wright, P. E. (1988) *Inorg. Chem. 27*, 2306−2312.

Moore, J. M., Case, D. A., Chazin, W. J., Gippert, G. P., Havel, T. F., Powls, R., & Wright, P. E. (1988a) *Science 240*, 314−317.

Moore, J. M., Chazin, W. J., Powls, R., & Wright, P. E. (1988b) *Biochemistry 27*, 7806−7816.

Moore, J. M., Lepre, C. A., Gippert, G. P., Chazin, W. J., Case, D. A., & Wright, P. E. (1991) *J. Mol. Biol. 221*, 533−555.

Nilges, M., Clore, G. M., & Gronenborn, A. M. (1988) *FEBS Lett. 229*, 317−324.

Pladziewicz, J. R., & Brenner, M. S. (1987) *Inorg. Chem. 26*, 3629−3634.

Plateau, P., Dumas, C., & Guéron, M. (1983) *J. Magn. Reson. 54*, 46−53.

Rance, M. (1987) *J. Magn. Reson. 74*, 557−564.

Rance, M., Sørensen, O. W., Bodenhausen, G., Wagner, G., Ernst, R. R., & Wüthrich, K. (1983) *Biochem. Biophys. Res. Commun. 117*, 479−485.

Redfield, A. G., & Kunz, S. D. (1975) *J. Magn. Reson. 19*, 250−254.

Redinbo, M. R., Cascio, D., Choukair, M. K., Rice, D., Merchant, S., & Yeates, T. O. (1993) *Biochemistry 32*, 10560−10567.

Rush, J. D., Levine, F., & Koppenol, W. H. (1988) *Biochemistry 27*, 5876−5884.

Shaka, A. J., Barker, P. B., & Freeman, R. (1985) *J. Magn. Reson. 64*, 547−552.

Shaka, A. J., Lee, C. J., & Pines, A. (1988) *J. Magn. Reson. 77*, 274−293.

Sykes, A. G. (1985) *Chem. Soc. Rev. 14*, 283−315.

Sykes, A. G. (1991) *Adv. Inorg. Chem. 36*, 377−408.

Sørensen, O. W., Rance, M., & Ernst, R. R. (1984) *J. Magn. Reson. 56*, 527−539.

Vuister, G. W., Boelens, R., & Kaptein, R. (1988) *J. Magn. Reson. 80*, 176−185.

Wagner, G., & Brühwiler, D. (1986) *Biochemistry 25*, 5839−5843.

Wagner, G., Braun, W., Havel, T. F., Schaumann, T., Gõ, N., & Wüthrich, K. (1987) *J. Mol. Biol. 196*, 611−639.

Wijmenga, S. S., & van Mierlo, C. P. M. (1991) *Eur. J. Biochem. 195*, 807−822.

Wishart, D. S., & Sykes, B. D. (1994) *Methods Enzymol. 239*, 363−392.

Wolk, C. P. (1980) in *The Biochemistry of Plants. A Comprehensive Treatise. Vol. 1. The Plant Cell* (Tolbert, N. E., Ed.) pp 659−686, Academic, New York.

Wüthrich, K. (1986) *NMR of Proteins and Nucleic Acids*, Wiley, New York.

Wüthrich, K., Billeter, M., & Braun, W. (1983) *J. Mol. Biol. 169*, 949−961.

BI960621Y